Self-rolled-up microtube ring resonators: a review of geometrical and resonant properties

Xiuling Li

Department of Electrical and Computer Engineering, Micro and Nanotechnology Laboratory, University of Illinois, Urbana, IL 61801, USA
xiuling@illinois.edu

Received June 10, 2011; revised November 1, 2011; accepted November 1, 2011; published December 5, 2011 (Doc. ID 149107)

Strain-induced self-rolled-up microtubes, a category of recently discovered tubular structure with ultrathin walls, have been demonstrated to be unique ring resonators. Recent development in their geometrical and resonant properties are reviewed. © 2011 Optical Society of America

OCIS codes: 070.5753, 140.4780, 230.5750

Self-rolled-up microtube ring resonators: a review of geometrical and resonant properties

Xiuling Li

Introduction

Optical microring resonators, confining light to circulate in tight bends via the whispering gallery effect, have shown themselves to be ideal candidates for applications including optical signal processing and biosensing [1,2]. Conventional methods to fabricate resonant optical microcavities of various shapes and dimensions mostly involve multilevel lithography and dry etching. Microdisks, toroids, rings, etc., both passive and active cavities with resonance frequencies in visible and IR wavelengths, have been demonstrated to have super-high quality factors and extremely fine spectral resolution [1]. Common issues with the fabrication process includes sidewall roughness due to ion damage associated with dry etching, a limited capability of realizing active microcavities of desired dimensions, and challenges in structure designs for mode overlaps as well as uniformity and precision for coupled arrays. Recently, strain-induced self-rolled-up tubular structures, first discovered by Prinz *et al.* [3], with tube wall thicknesses typically below ~200 nm and diameter ~1–10 μm, have been demonstrated to be effective microcavities, bearing optical resonant modes in the visible and infrared wavelength range [4–7]. Note that although the diameter and tube length are in the range of micrometers, the tube wall thickness is well below the wavelength of the optical modes. The tube walls can be epitaxially smooth. The active media epitaxially incorporated into the tube wall naturally overlap with the maximum optical field intensity. Several reviews have been published on the fabrication process as well as optical characteristics of the formed cavities [8–16]. The present paper attempts to review the most recent results of the fabrication, transfer, and optical characterization of self-rolled-up microtube ring cavities. The cavities include those fabricated either from epitaxial semiconductor or dielectric membranes with self-embedded quantum-dot (QD), quantum-well (QW) active gain regions, as well as external light emitters in the evanescence field of the ultrathin wall. The application of this new paradigm, both as individual cavities and potentially in an array fashion, will be discussed. This paper is organized to include two major sections: (1) geometrical characteristics of rolled-up membrane tubes, and (2) resonant characteristics of optically active rolled-up microtube cavities.

Figure 1

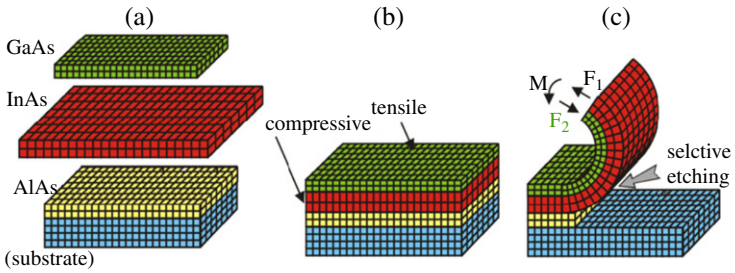

Schematic illustration of the mechanism of strain-induced deformation of membranes. (a) GaAs/InAs bilayer structure with AlAs as the sacrificial layer, where InAs has a larger lattice constant than GaAs. (b) The bilayer is pseudomorphically deposited on the substrate; InAs experiences compressive strain and GaAs experiences tensile strain. (c) Selectively removing the AlAs sacrificial layer releases the bilayer, and a net momentum derived from the opposite force from each of the bilayers drives the membrane to curve and roll into tubes. Adapted from [3].

1. Geometrical Aspects of Self-Rolled-Up Tubular Structures

Strain-induced self-rolled-up tubes are formed spontaneously when strained planar membranes deform driven by energy relaxation, first discovered by Prinz *et al.* in 2000 [3]. An example of such a self-rolling phenomenon is illustrated in Fig. 1 using a GaAs–InAs bilayer system. The InAs layer is compressively strained when pseudomorphically deposited on a GaAs substrate. When it is released from the substrate by selective removal of the AlAs sacrificial layer, the InAs layer has the tendency to expand, while the GaAs layer resists the expansion. The opposite force from each of the bilayers generates a net momentum, driving the planar membrane to scroll up and continue to roll into a tubular spiral structure as the sacrificial layer is etched laterally. By combining lithographic patterning and subsequent epitaxial liftoff of the membrane, site control of these rolled-up tubes can be realized. Depending on the shape, geometry, and crystal orientation of patterned membranes, the released membranes can deform into tubes, coils, hinges, and rings [10,17–19]. The curvature of self-rolled-up semiconductor tubes is proportional to the mismatch strain of the membrane. The number of rotations can be controlled by predefining the size and shape of the membranes before rolling up. As long as the thin membrane is strained and can be released from its mechanical support, self-rolled-up tubes will form spontaneously, as has been demonstrated for III–V compound semiconductor systems including GaAs, InP, and GaN, elemental semiconductors of Si and Ge, and metal and dielectric materials.

Figure 2

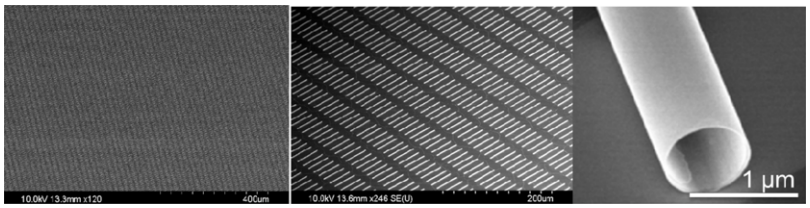

Scanning electron microscope (SEM) images of wafer scale ordered array of $In_{0.30}Ga_{0.7}As$/GaAs bilayer microtubes, with increasing magnification from left to right.

1.1. Rolling-up Strained Semiconductor Membranes by Epitaxial Liftoff

In semiconductor materials system, residual strain in a thin membrane can be precisely controlled by growing lattice mismatched epitaxial films using either metalorganic chemical vapor deposition (MOCVD) or molecular beam epitaxy (MBE). Extensive reviews on the effect of strain, crystal orientation, and membrane geometry on the rolling behavior and mechanism of strained epitaxial semiconductor films have been published previously [8, 15]. Briefly, the typical mismatch strain for III–V compound semiconductors is ~1%–10%; thus for total film thicknesses of 1–100 nm, the tube diameter would be in the range of ~10 nm to 10 μm. The smallest diameter nanotube that has been demonstrated is ~3 nm, using one monolayer (ML) of InAs and one ML of GaAs, which has a mismatch strain of 7.16% [1,8]. Shown in Fig. 2 is an array of highly ordered $In_{0.3}Ga_{0.7}As$–GaAs bilayer rolled-up tubes that are 0.6 μm in diameter, 50 μm in length, and 12 nm in wall thickness. Coherent InAs quantum dots (QDs) embedded in strained $In_{0.68}Ga_{0.32}As_{0.41}P_{0.59}/In_{0.81}Ga_{0.19}As_{0.41}P_{0.59}$ membranes grown on InP substrate have been reported to roll up into microtubes that emit at 1.55 μm by selectively etching the InP substrate [20]. Ultrathin crystalline AlN/GaN nanomembranes epitaxially grown on Si(111) have been demonstrated to self-assemble into tubes, spirals, and curved sheets when released through the selective etching of the silicon substrate [21]. Yu *et al.* [22] recently fabricated curled 3D objects from epitaxial Si on silicon-germanium-on-insulator (SiGeOI) driven by lattice mismatch between Si and Ge. They further demonstrated mechanical actuation by applying liquid to partially open the curls.

1.2. Rolling-up Strained Dielectric, Metal, and Hybrid Nonepitaxial Membranes

In addition to epitaxial liftoff of strained semiconductor membranes, releasing and rolling-up strained dielectric films (e.g., SiN_x or SiO_x) from their mechanical support has also been achieved. As reported by Mei *et al.* [23], dielectric tubes can be formed by using photoresist (polymer) as the sacrificial layer on a glass substrate, taking advantage of the extremely good chemical etching selectivity of inorganic versus

organic materials using acetone. This method successfully produced rolled-up tubes made of various materials and material combinations, including SiO/SiO_x, Pt, Pd/Fe/Pd, TiO_2, ZnO, Al_2O_3, Si_xN_y, Si_xN_y/Ag, and diamond-like carbon (DLC).

Chern *et al.* developed a method to fabricate rolled-up metallic or metallic and dielectric hybrid microtubes [24]. Ordered arrays of Au microtubes with diameters in the range of ~1–3 μm, controlled by layer thickness, were demonstrated by depositing Au (presumably strained along surface normal) on top of a Ag film on a silicon substrate. Au spontaneously deforms into tubular shapes once the bottom Ag film is delaminated from Au through metal assisted chemical etching (MacEtch) of Si [25].

In contrast to epitaxial film, where the strain can be precisely controlled by material composition (such as the In% in $In_xGa_{1-x}As$ film) and thickness, the strain mechanism in nonepitaxial films is more complicated and less controllable. As a result, deposition conditions including rate, frequency, temperature, and background pressure affect the strain in the deposited films through thermal expansion coefficient differences and stress evolution during deposition. Strain engineering is required in nonepitaxial films by optimizing the deposition conditions, in order to enhance the strain gradient within the nanomembranes to achieve uniform controllable diameters. However, the range of diameters achievable is still limited for certain materials. Nonetheless, the methods of rolling up nonepitaxial membranes allow low-cost alternatives to fabricating tubular structures using strained epitaxial layers, either as rolling vehicles to bring other materials or structures onto curved surfaces, or as active cavities for resonators. These methods also open up heterogeneous integration of diverse materials and novel material combinations for potential applications in, e.g., metamaterials [23,26–28], optical signal processing, and optofluidics [29].

1.3. Rolling-up Patterned Strained Membranes to Form Holey or Nanoporous Tubes

In addition to regular solid layer of strained thin film membrane, patterned membranes can be rolled up by the same mechanism, and the patterns do not seem to affect the tube diameter or integrity. We previously reported [30] holey tubes formed from rectangular-shaped thin films with periodic holes patterned before the film was rolled up. The periodic array of holes not only serves as etching holes for faster release of the thin film from the substrate, but also adds functionality to the tubes. Microtubes with holes patterned by photolithography not only do not degrade, but also enhance the photoluminescence intensity, probably because of better external coupling efficiency [30]. Curved periodically patterned photonic structures can have implications in novel photonic device concepts.

The rolled-up microtubes can be made porous by depositing Au on the rolled-up tubes and immersing them in a metal-assisted chemical etching (MacEtch) solution [25,31–34]. Shown in Fig. 3(b) are InGaAs–GaAs rolled-up tubes with nanoporous walls. Not surprisingly, when too many holes are drilled, the tube tends to collapse as shown in Fig. 3(c). Mei *et al.*

Figure 3

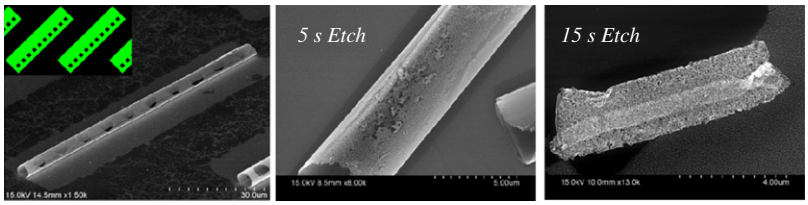

(a) SEM images of rolled-up $In_{0.3}$ $Ga_{0.7}$ As–GaAs microtubes with periodic holes patterned before rolling. Insets show the membrane pattern. Porous InGaAs–GaAs microtubes formed by metal assisted chemical etching for (b) 5 s and (c) 15 s after rolling up the tube. Adapted from [30, 32].

recently reported nanoporous crystalline GaN/AlN microtubes with pore sizes ranging from several to several tens of nanometers from initial island growth of AlN on Si(111) [21].

1.4. Deterministic Assembly, Transfer, and Integration of Rolled-up Microtubes

The self-rolling direction is influenced by the elastic anisotropy in A3B5 cubic crystals. For $In_xGa_{1-x}As$–GaAs materials, the crystal is less stiff along ⟨100⟩ directions than along ⟨110⟩ directions. For crystallographically equivalent directions, the final rolling direction depends on the length and width of the membrane as well as on the diameter of the rolled-up tubes, as confirmed by both experimental and theoretical studies [17,35]. The energetics of the final state, the history of the rolling process, and the kinetic control of the etching isotropy are all factors contributing to the rolling behavior. The revelation of these governing mechanisms as well as the guidelines provided have significant impact on the precise site and direction control of tubular and curved semiconductor nanostructures. Wafer scale extremely ordered tubes with uniform diameters have been demonstrated, as shown in Fig. 2.

Z. Mi's group has reported [36] a controlled transfer of a single rolled-up semiconductor microtube from its host substrate to a foreign one by inserting the abrupt tapers of an optical fiber into two ends of the tubes and lifting off the rolled-up microtubes. They have successfully transferred a QD microtube onto the cleaved facet of a single-mode fiber and a silicon substrate and demonstrated strong coherent emission from the transferred tubes, as shown in Fig. 4.

X. Li's group has done some initial exploration of heterogeneous integration of rolled-up tubes with other substrates by transfer-printing, a technology pioneered by Rogers and co-workers [37], without altering the spatial alignment on host substrates. This is an array-based integration technology, which has the potential to faithfully maintain not only the alignment, but also the registry of the tubes. Figure 5(a) shows the transfer result of an $In_{0.2}Ga_{0.8}As$/GaAs microtube array from GaAs substrates to a poly (dimethyl siloxane) (PDMS) stamp. The integrity of the rolled-up tubes has mostly been maintained after transfer (Fig. 5(b)).

Figure 4

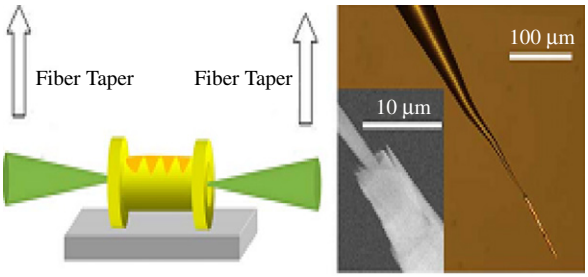

Transfer of rolled-up microtubes using tapered optical fiber. (a) Illustration of the liftoff of a microtube device from the host GaAs substrate. (b) Optical microscopy and SEM (inset) images of a tube attached to the tip of a fiber during the transfer process. Reproduced with permission from Ref. [36].

It can be seen from Fig. 5(c) that the tubes have been completely removed from the native GaAs substrate, where the color contrast indicates GaAs height difference between the stripes (lighter color) where the tubes were located and the trenches (darker color) where undercutting etching took place. This capability opens up the prospect of using rolled-up tubes as building blocks for flexible nanoelectronic and nanophotonic applications. Further, the density of the tubes can be increased by printing multiple times and placing the tubes in a staggered fashion. The layer formed from the transferred tubes can also be placed deterministically to fit the needs of, e.g., a phased array to be integrated with other optical components in integrated photonic circuits on the desired receiving substrates.

2. Resonant Characteristics of Self-Rolled-up Microcavities

2.1. Optically Active Media for Rolled-up Microtubes

Optically active structures including quantum wells (QWs) and QDs can be rolled up by using the strained $In_xGa_{1-x}As$ layer as a wrapper while keeping the rest of the layers either lattice matched to the substrate or involving discrete structures. Figure 6 illustrates three types of active media that can be epitaxially incorporated in the tube wall.

Film growth for the rolled-up active structures is the same as growing planar device structures, except the design involves much thinner layers; e.g., the AlGaAs barrier layer in the examples illustrated in Fig. 6 is typically in the range of 5–20 nm, in contrast to ~300–1000 nm thick cladding layers for a conventional edge-emitting laser structure. Despite that, intense photoluminescence (PL) signals (Fig. 7) have been observed that are approximately one order of magnitude stronger than their planar counterparts, as reported by Chun *et al.* for rolled-up 5 nm GaAs QW with 10 nm AlGaAs clad layers on each side [30]. The same intensity enhancement behavior was previously reported for tubes consisting of

Figure 5

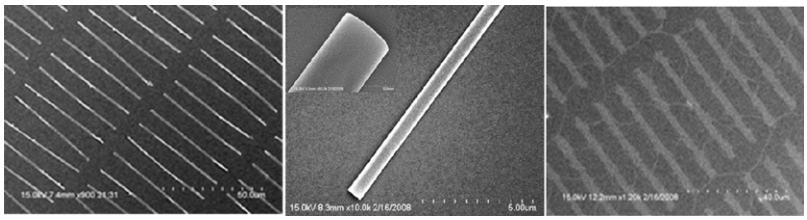

Transfer printing of an InGaAs–GaAs microtube array. From left to right, SEM images of transferred tubes on PDMS; enlarged images of a tube on PDMS after transfer, showing the integrity of the tube; and the host GaAs substrate after tubes are transferred.

Figure 6

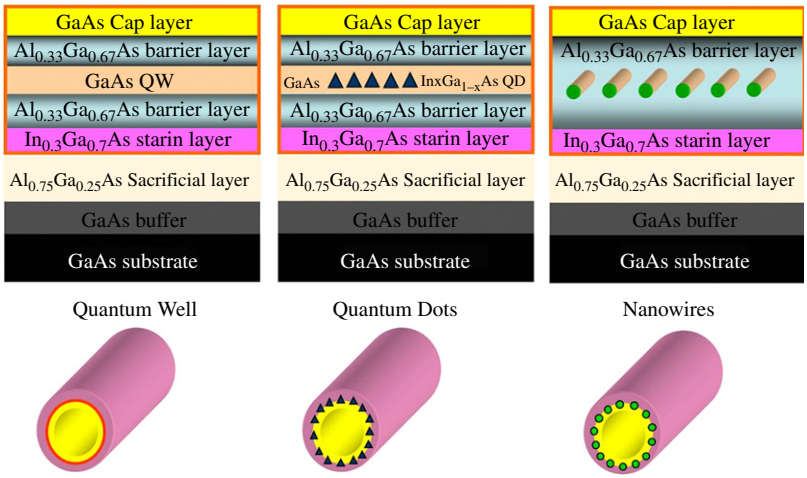

Illustration of rolled-up tubes with epitaxial QW, QD, and nanowires as the active media. Reproduced with permission from [9].

a 3 nm type II GaAs QW that was transitioned to type I after rolling up [38]. Patterning the rolled-up QW tubes with periodic holes further enhanced the PL intensity [30]. In addition to PL intensity enhancement, the curved QW showed peak shift as a function of the tube diameter, consistent with strain-induced bandgap shift—demonstrating the effect of curvature, another degree of freedom in addition to composition and thickness for tuning semiconductor fundamental parameters [30].

Self-assembled Stranski–Krastanov InAs or InGaAs QDs grown on GaAs or InP substrates have been incorporated into the tube walls by molecular beam epitaxy (MBE) [20,39–41]. Low absorption losses of InAs QDs due to 3D confinement and low density of states, in contrast to QW structures, combined with surface corrugation for better axial confinement, led to the demonstration of optically pumped microtube lasers, which will be further discussed below [5].

In addition to epitaxial active media, Si nanocrystals formed by annealing SiO_x/Si thin film emitting in the visible wavelength range have been

Figure 7

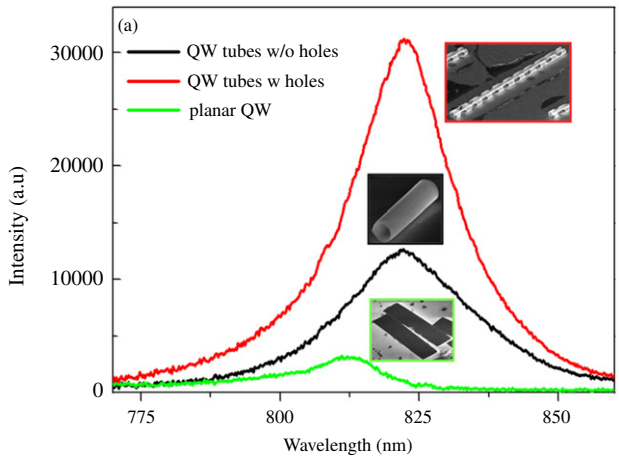

PL spectra from a 5 nm GaAs QW structure before and after rolling up, as well as rolled-up tubes with periodic holes patterned in the tube wall.

effectively used as the active media for the hybrid material microtube ring resonators [4]. Furthermore, instead of monolithically incorporating active media into the tube wall, Dietrich *et al.* demonstrated optical modes in rolled-up microtube resonators that are excited by PbS nanocrystals filled into the microtube core [42]. Long-ranging evanescent fields in the very thin walled microtubes cause strong emission of the nanocrystals into the resonator modes and a mode shift after self-removal of the solvent.

2.2. Suspending Microtubes to Reduce Radiative Loss to Substrate

To reduce radiative loss through the substrate, the tubes must be free-standing. A U-shaped mesa, first demonstrated by Kipp *et al.* [6], has been effectively used to suspend the middle of the microtube from the substrate. As summarized by Mi *et al.* [12], the fabrication procedure consists of the following steps: (1) lithographically define a U-shaped membrane down to the strained InGaAs; (2) deep etch pass the AlAs sacrificial layer inside the two arms of the U shape, which serve as the air bridge for the rolled-up tube later on and define the suspended height of the eventually rolled-up tube; (3) broad shallow etch to the sacrificial layer to define the rolling edge; and (4) use HF to release the patterned membrane to roll into a dumbbell shape, as shown Fig. 8. Clear mode-like peaks have been observed by using these free-standing rolled-up tubes with QDs.

2.3. Radial and Axial Modes and Design Considerations for Confinement

In optical ring resonators, the whispering gallery modes form owing to total internal reflection of light at the boundary between the high- and

Figure 8

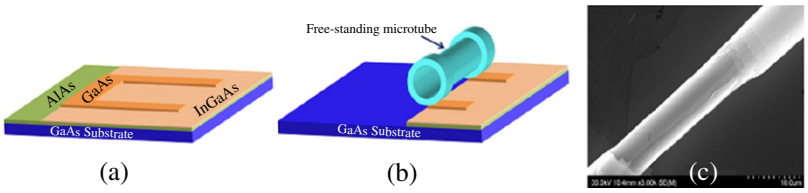

(a), (b) Illustrations of the formation of free-standing rolled-up microtubes using a U-shaped mesa. (c) SEM image of the rolled-up tube formed by using the illustrated procedure. Reproduced with permission from [12].

low-refractive-index media. In microtube ring resonators, in addition to modes arising from photons circulating around the tube circumference (azimuthal modes), axial modes resulting from light oscillating back and forth along the tube axis for finite length tubes are also supported. The emission spectra exhibiting sharp peaks with superposition of azimuthal and axial modes are characterized by several groups.

For the azmuthal modes, the optical resonance has to satisfy the azimuthal phase matching condition, described by $n_{\text{eff}}L = \lambda m$, where L is the circumference of the microtube, n_{eff} is the effective refractive index, λ is the vacuum wavelength of the propagating light, and m is the azimuthal mode number. The modelike peaks, sharp and equally spaced with each peak corresponding to an integer value of the azimuthal mode number m, are superimposed onto the broad luminescence band of the active media (QWs or QDs). Degeneracy between clockwise and counterclockwise propagating wave packets is lifted by the radial asymmetry of the tube circumference, where the wall thickness undergoes a sudden change at the inner and outer edges of the rolled-up tubes. This has been observed by Mi's group [12] as shown in Fig. 9, where the two nondegenerate modes can be clearly seen.

Structural variations along the axial length of the tube at the rolling edges, such as a lobe or sinusoidal corrugation, where the modes are confined, can significantly change the axial field distribution. These surface features represent locally increased or decreased winding numbers of the rolled-up tube. Strelow *et al.* demonstrated [43] using spatially resolved PL spectra and mapping at low temperature, that the axial modes in microtubes can be controlled precisely by the shape of the lobes in their rolling edges. The lobe size in these structures is of the order of a few to ~10 μm at the widest part. As shown in Figs. 10(a) and 10(b), both the triangular- and the rectangular-shaped lobes, patterned on the rolling edge of InAlGaAs rolled-up tubes with InAs QDs embedded, produced groups of axial modes. The mode spacings are in direct accordance with the electronic counterparts of differently shaped potentials. The axial modes for the rectangular lobe are much weaker, and the spacing is much smaller. Strelow *et al.* also fitted the experimental data with excellent agreement by finite-difference time domain simulation using an adiabatic separation of the circulating and axial propogation and extracting exact geometry from SEM images. Mi's group [41] incorporated periodic surface corrugations in the shape close to parabola that are ~5 μm in width and ~5 μm in height in their

Figure 9

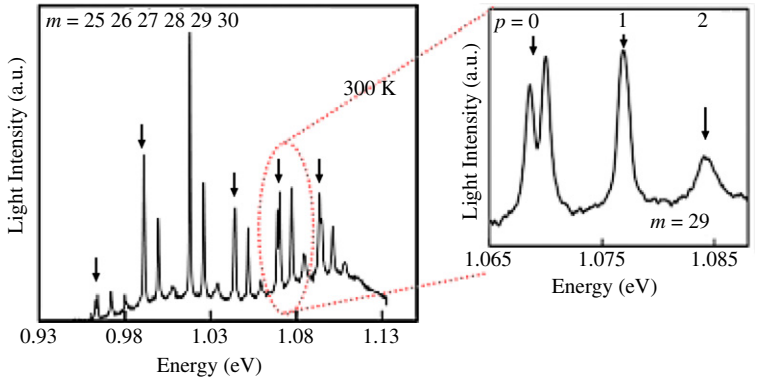

Nondegeneracy of azimuthal modes. PL spectrum measured from a freestanding InGaAs/GaAs QD microtube with surface corrugations at room temperature. The corresponding azimuthal mode numbers ($m = 25$–30) are labeled. A detailed view of the eigenmodes associated with azimuthal mode number $m = 29$ is shown in the inset, wherein the axial mode numbers are identified as $p = 0, 1, 2$. The two nondegenerate modes associated with $p = 0$ are induced by the inside and the outside rolling edges around the tube. Adapted from [12].

Figure 10

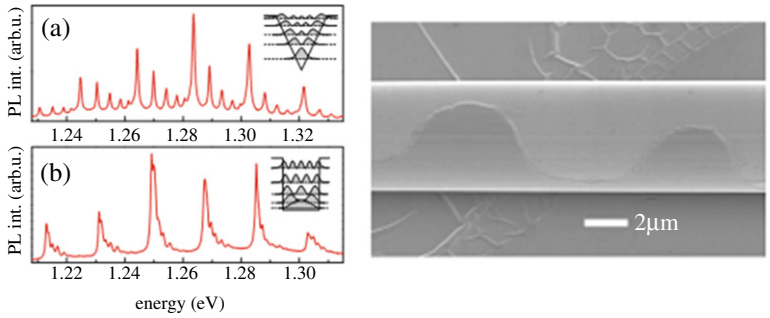

Effect of surface geometry. Resonant mode peaks from InGaAs QD microtubes with (a) triangular and (b) rectangular surface geometry at the outer edge of the rolling edges, respectively, reproduced with permission from [43]. The SEM image on the right shows clear periodic surface corrugation, reproduced with permission from [41].

InGaAs QD rolled-up tube structures, as shown in Fig. 10(c). For tubes that are <20 μm in length, only ~2 notches, not exactly evenly spaced or uniform in height, are contained in the free-standing part of the tube. It is by using this structure that optically pumping lasing action was achieved by Mi's group (more discussion of lasing is presented below).

Figure 11

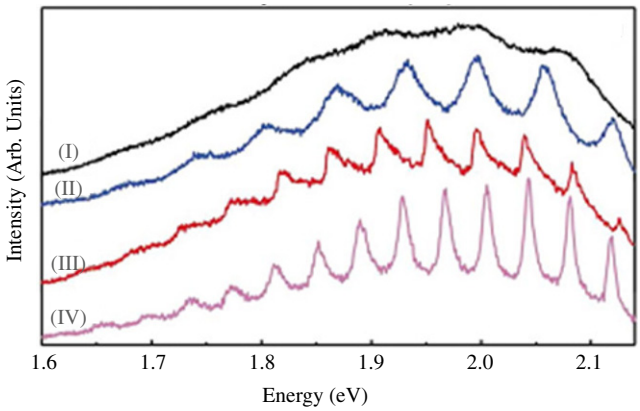

PL spectra from microtubes of (I) 27, (II) 33, (III) 40, and (IV) 45 nm in wall thickness (corresponding diameters are ~4–9 μm), showing stronger and narrower resonance peaks with increasing thickness. Reproduced with permission from [7].

2.4. Tuning the Resonant Modes

Mode position and intensity can be tuned by the number of rotations, film thickness, and local environment, all of which change the effective refractive index or index contrast.

2.4a. Effect of Varying Tube Wall Thickness by Increasing Film Thickness

As shown in Fig. 11, Bolaños Quiñones *et al.* demonstrated [7] that by increasing the wall thickness of rolled-up SiO/SiO_2 tubes, which in turn changes the tube diameter, the resonant modes become more pronounced. When the wall thickness is thinner than 27 nm, resonant modes become practically unobservable, which is attributed to the dominance of light diffraction over the modes propagation in the tube wall.

2.4b. Effect of Varying Tube Wall Total Thickness by Multiple Rotations

The Mi group [44] studied the effect of the number of rotations for an InGaAs QD rolled-up tube resonator. The light scattering effect and, consequently, the Q factors, depend strongly on the number of revolutions. For a 5 μm diameter tube with wall thickness of ~50 (single rotation) and 200 nm (four rotations), the mode peaks became noticeably narrower with increasing total thickness, especially from single turn to double turn. Q factors of ~6000 and 40,000 have been calculated by finite-difference time domain simulation for ~1 and 4 revolutions. The energy separations between the adjacent azimuthal modes are ~24, 21, and 19 meV, and the energy separations between the adjacent axial modes are ~7, 4, and 2–3 meV, for microtubes with wall thicknesses of ~50, 100, and 200 nm, respectively.

Figure 12

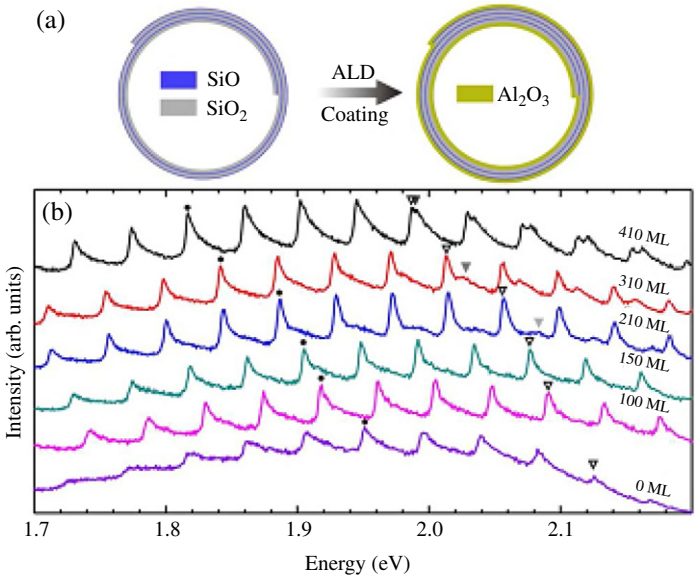

(a) Schematic cross-section diagram of an SiO/SiO_2 microtube before and after atomic layer deposition coating with As_2O_3. (b) PL spectra for various microtubes with different Al_2O_3 thickness in monolayers (MLs) as labeled.

The effect observed here is very similar to varying the wall thickness by increasing rolling film thickness, except the latter changes the tube diameter much more than the former, which induces more strain-related peak shifts.

2.4c. Effect of Varying Tube Wall Thickness by Post-Tube-Fabrication Deposition

In addition to the film thickness and the number of rotations, the tube wall thickness can also be tuned by post-tube-fabrication dielectric deposition. It has been demonstrated that Al_2O_3 deposited by atomic layer deposition (ALD), which coated the inside and outside of the tubes conformably, can be used to coarse and fine tune the properties of SiO/SiO_2 rolled-up optical ring resonators after their fabrication [7]. As shown in Fig. 12, the intensity of mode peaks appears to increase, and peak positions can be smoothly shifted over a wide spectral range as a function of Al_2O_3 thickness. After 210 ML coating, new shoulder peaks, which could be axial modes, start to be resolved. Similarly, HfO_2 effectively improves the light confinement further, compared with the Al_2O_3 coating, since HfO_2 has a larger refractive index [45].

2.4d. Applications in Optofluidic Sensing

The ultra-thin (subwavelength) walled microtube ring resonator can be used for optofluidic sensing and potentially for lab-on-a-chip applications, such as real-time bioanalytic systems.

When the light energy cannot be completely confined in the resonator wall of the high-refractive-index medium, the evanescent field penetrates into the low-refractive-index medium and interacts with the materials near the interface, leading to a wavelength shift of the light circulating in the optical ring resonator. Thus, sensing applications of ring resonators are realized by simply detecting spectral shifts of the optical resonant modes. Huang *et al.* [45] studied the effect of surrounding liquid on the resonant behavior of SiO/SiO_2 rolled-up tubes. Their spectral peak positions shift significantly when measurements are carried out in different surrounding liquids. Analytical calculations as well as finite-difference time-domain simulations are performed to investigate the light confinement in the optical microcavities numerically and to describe the experimental mode shifts very well. A maximum sensitivity of 425 nm/refractive index unit (RIU) is achieved for the microtube ring resonators. In contrast, conventional optical microcavity-based sensors derived from glass capillaries typically have a tube diameter and wall thickness about 10 times larger and sensitivity of less than 35 nm/RIU [45]. The higher sensitivity is attributed to the pronounced propagation of the evanescent field in the surrounding media due to the subwavelength wall thickness design of the microcavity. The authors also indicated that the sensitivity can be further enhanced by operating the sensors in a longer wavelength range (i.e., smaller azimuthal numbers, fewer nodes, effectively weaker confinement), since the diffraction loss is much more prominent in the field pattern of the mode with lower azimuthal numbers. On the other hand, the reduced thickness weakens the light confinement and thus lowers the Q factor in the resonator, hindering the device from sensing tiny changes of refractive index, and a detection limit of around 10^{-4} RIU was reported. The Q factor could be improved by incorporating surface features such as periodic corrugation such in the case of Ref. [46]. However, for sensing large changes of refractive index, the high sensitivity of the rolled-up microcavities provides a cheap and simple way to produce large spectral shifts for detection.

2.5. Polarization and Directional Emission

Polarization-dependent PL measurements revealed two groups of modes, which were identified as transverse electric (TE) modes (along the tube axis) and transverse magnetic TM modes (perpendicular to the tube axis). For the optically pumped 1240.7 nm lasing peak in InGaAs QD microtube demonstrated by Li *et al.*, the lasing mode appears 100% TE polarized based on measurement of the intensity of the lasing mode as a function of polarization angle. The TE modes only exist in microtube ring resonators with thick walls (thus small diffraction loss).

When the microtubes are immersed in the liquids, as reported by Huang *et al.* [45], the TE modes were almost undetectable. This is because the higher refractive indices of the surrounding liquids increase the light loss for both TM and TE modes, but the loss for TE modes is much more prominent than for the TM modes.

Because of the existence of inner and outer rolling edges, rolled-up microtube devices offer distinct advantages of directional preferential

Table 1. Geometrical and Resonant Properties of Self-Rolled-up Microtubes

Geometrical Attributes	Resonant Characteristics
Nanometer scale ultra-thin wall	Subwavelength emission in one of the dimensions (wall thickness); Low Q factor; Pronounced light diffraction and evanescent field propagation into the surrounding low-refractive-index medium.
Deterministic diameter in micrometer range	Continuous tuning of resonant modes by wall thickness and diameters
Active gain material and surface structures readily embedded	External coupling may not be required
Smooth side walls for epitaxially strained membranes	Reduced scattering loss
Existence of inner and outer edges	Weak confinement factor leading to low Q factor; Preferential light output from the inner rolling edge
Ease of fabrication of high-aspect-ratio tubes (e.g., long and narrow tubes) with surface structures at rolling edges	Axial and radial confinement and distribution of light
Large area array	Phased array for integrated photonic circuits possible
Heterogeneous integration	III–V optical devices and circuits on Si CMOS feasible

emission at a defined position on the tube as well as controlled output coupling efficiency. As clearly demonstrated experimentally [43,47], the inside edge of the rolled-up tube predominantly emits optical resonance modes, while the outside edge emits only leaky modes. Such directional emission can also be visualized by the simulated electric field distribution of the resonance mode in a microtube where the inner edge and the outer edge do not overlap. This property makes the microtube ring laser a good candidate for a directional light source on a chip, since the direction of the laser light can be adjusted by controlling the relative position of inside and outside edges.

Table 1 summarizes the geometrical attributes and the corresponding resonant properties discussed.

2.6. Optically Pumped Lasing

Remarkably, room temperature lasing has been demonstrated by Z. Mi's group from strained InGaAs/GaAs QD rolled-up tubes pumped by a 633 nm He–Ne laser at room temperature [5]. As shown in Fig. 13, with the increase of pump power, a linewidth reduction from ~0.6–0.8 nm to ~0.4–0.5 nm is observed, which corresponds with the measured threshold, further confirming lasing from the microtube cavity. A small increase of the spectral linewidth at higher pump powers is also present, possibly due to a heating effect. An ultralow threshold of ~4 μW was estimated from integrated emission intensity versus pump power plot. Considering the spot size of the pump laser, the threshold density is ~400 W/cm^2.

Figure 13

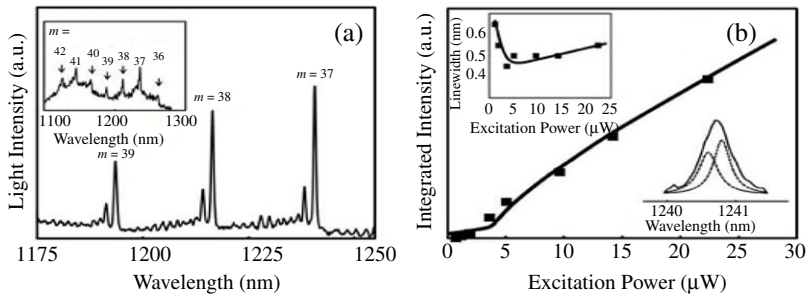

(a) Room temperature emission spectrum of InGaAs/GaAs QD microtube measured at above-threshold pump power (~23 μW) and below threshold (inset). (b) Integrated light intensity for lasing mode at 1240.7 nm versus excitation power, with a detailed view of the lasing peak at 1240.7 nm fitted with two Lorentzian curves (lower inset) and linewidth dependence (upper inset). Reproduced with permission from [5].

2.7. Towards Electrical Injection

In order to achieve electrical injection, doping and contact issues must be addressed. Doping of these structures compared with most other nanostructured devices is straightforward, since doping can be done in the planar structure by using traditional epitaxial doping methods. Some metal contacts can also be formed before rolling up [48,49]. Mi's group demonstrated their efforts on electrical pumping of rolled-up tube structures of InGaAs QD tubes [44]. The epitaxial structure is doped with Si in the top and Be in the bottom barriers (at least 20 nm is needed to avoid depletion at maximum doping level). The contact scheme of n-metal and p-metal and the fully fabricated device are shown in Fig. 14. The tube is cast in SU-8, so that the p-metal can be reached by finger contact from outside of the tube, and n-metal can be outside of the rolled-up part. Note that the n-metal and p-metal are not in the same plane; they are separated by approximately the tube height, which could be challenging to fabricate, since the SU-8 pedestal height has to be just right to avoid stressing the finger contact. With the p-contact placed directly near the device active region, the device resistance and heating effect can be drastically reduced; on the other hand, radiative loss to the metal layer is not desired. The resulting electrical contact is not Ohmic yet, as is shown in Fig. 14 (bottom left). After metal contacts are formed, the sharp mode peaks changed to broad peaks with much lower Q factors under the same optical pumping condition (Fig. 14, lower right). The effort of Mi's group represents an important step towards the realization of electrical injected rolled-up microtube ring resonators.

In summary, this paper presented a brief overview of a new tubular architecture that is formed by self-rolling of strained semiconductor heterojunction or dielectric hybrid membranes and its characteristics as ring resonators with embedded optical gain medium in or near the tube wall. The fabrication method that combines top-down lithography with bottom-up growth and deposition for strain engineering, as well as the capability for heterogeneous integration, makes the rolled-up

Figure 14

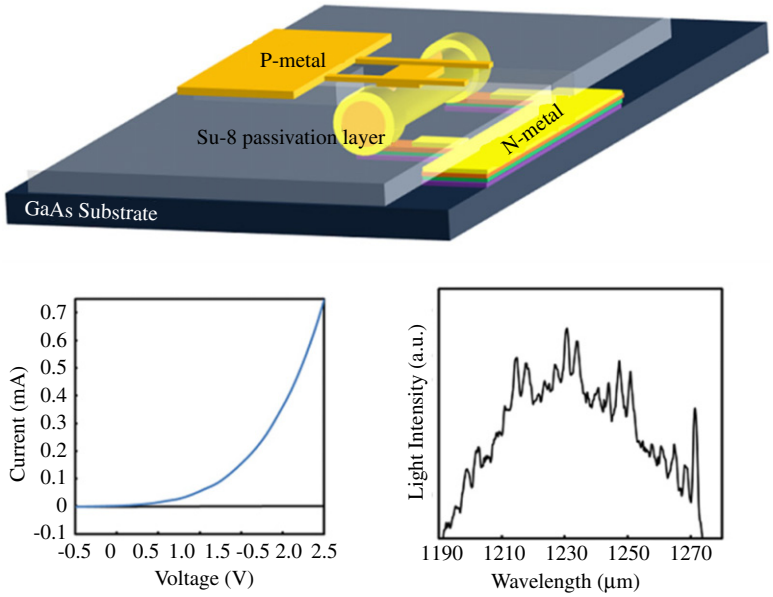

Electrically injected InGaAs QD microtube. Top: schematic of the electrical contact scheme. N-metal is deposited on the two side pieces of the mesa. SU-8 is used as the passivation layer, and the p-metal contact is placed directly on the microtube top surface. Bottom: I–V chracteristics measured, showing rectifying behavior; and emission spectrum under *optical* pumping. Adapted from [44].

tubes good candidates for array-based photonic applications. The fine tunability, which is essential for realizing optical microdevices, brings a better understanding of the resonant modes in microtubular cavities and makes rolled-up tubes a powerful building block for photonic systems. Although many challenges still lay ahead, this new platform, consisting of a curved and optically active surface, is full of potential for discovering new fundamental physics as well as practical applications.

Acknowledgments

Support from NSF CAREER award 0747178 (ECCS) and NSF NSEC award 0749028 (CMMI) is acknowledged. Contributions by my students Ik Su Chun, Xin Miao, Karthik Balasunderam, Archana Challa, and Kevin Bassett are highly appreciated.

References and Notes

1. K. J. Vahala, "Optical microcavities," Nature **424**(6950), 839–846 (2003).
2. T. Ling and L. J. Guo, "Analysis of the sensing properties of silica microtube resonator sensors," J. Opt. Soc. Am. B **26**(3), 471–477 (2009).
3. V. Y. Prinz, V. A. Seleznev, A. K. Gutakovsky, A. V. Chehovskiy, V. V. Preobrazhenskii, M. A. Putyato, and T. A. Gavrilova, "Free-standing

and overgrown InGaAs/GaAs nanotubes, nanohelices and their arrays," Physica E **6**(1–4), 828–831 (2000).
4. R. Songmuang, A. Rastelli, S. Mendach, and O. G. Schmidt, "SiO_x/Si radial superlattices and microtube optical ring resonators," Appl. Phys. Lett. **90**(9), 091905 (2007).
5. F. Li and Z. Mi, "Optically pumped rolled-up InGaAs/GaAs quantum dot microtube lasers," Opt. Express **17**(22), 19933–19939 (2009).
6. T. Kipp, H. Welsch, Ch. Strelow, Ch. Heyn, and D. Heitmann, "Optical modes in semiconductor microtube ring resonators," Phys. Rev. Lett. **96**(7), 077403 (2006).
7. V. A. Bolaños Quiñones, G. Huang, J. D. Plumhof, S. Kiravittaya, A. Rastelli, Y. Mei, and O. G. Schmidt, "Optical resonance tuning and polarization of thin-walled tubular microcavities," Opt. Lett. **34**(15), 2345–2347 (2009).
8. X. Li, "Strain induced semiconductor nanotubes: from formation process to device applications," J. Phys. D Appl. Phys. **41**(19), 193001 (2008).
9. I. S. Chun, K. Bassett, A. Challa, X. Miao, M. Saarinen, and X. Li, "Strain-induced self-rolling III–V tubular nanostructures: formation process and photonic applications," Proc. SPIE **7608**, 760810 (2010).
10. O. G. Schmidt, C. Deneke, Y. M. Manz, and C. Müller, "Semiconductor tubes, rods and rings of nanometer and micrometer dimension," Physica E **13**(2–4), 969–973 (2002).
11. T. Kipp, C. Strelow, and D. Heitmann, "Light confinement in microtubes," in *Quantum Materials, Lateral Semiconductor Nanostructures, Hybrid Systems and Nanocrystals*, D. Heitmann, ed. (Springer, 2010), pp. 165–182.
12. Z. Mi, S. Vicknesh, F. Li, and P. Bhattacharya, "Self-assembled InGaAs/GaAs quantum dot microtube coherent light sources on GaAs and silicon," Proc. SPIE **7722**, 72200S (2009).
13. S. A. Scott and M. G. Lagally, "Elastically strain-sharing nanomembranes: flexible and transferable strained silicon and silicon–germanium alloys," J. Phys. D Appl. Phys. **40**(4), R75–R92 (2007).
14. V. Y. Prinz, V. A. Seleznev, A. V. Prinz, and A. V. Kopylov, "3D heterostructures and systems for novel MEMS/NEMS," Sci. Technol. Adv. Mater. **10**(3), 034502 (2009).
15. M. Huang, F. Cavallo, F. Liu, and M. G. Lagally, "Nanomechanical architecture of semiconductor nanomembranes," Nanoscale **3**(1), 96–120 (2011).
16. R. Stevenson, "Tube lasers prepare to light up silicon circuits," 2009, http://compoundsemiconductor.net/csc/features-details/19498536/Tube-lasers-prepare-to-light-up-silicon-circuit.html.
17. I. S. Chun, A. Challa, B. Derickson, K. J. Hsia, and X. Li, "Geometry effect on the strain-induced self-rolling of semiconductor membranes," Nano Lett. **10**(10), 3927–3932 (2010).
18. I. S. Chun and X. Li, "Controlled assembly and dispersion of strain-induced InGaAs/GaAs nanotubes," IEEE Trans. NanoTechnol. **7**(4), 493–495 (2008).
19. S. V. Golod, V. Y. Prinz, V. I. Mashanov, and A. K. Gutakovsky, "Fabrication of conducting GeSi/Si micro- and nanotubes and helical microcoils," Semicond. Sci. Technol. **16**(3), 181–185 (2001).
20. P. Bianucci, S. Mukherjee, P. Poole, and Z. Mi, "Self-organized 1.55 μm InAs/InP quantum dot tube nanoscale coherent light sources," in *2011 IEEE Winter Topicals (WTM)* (IEEE, 2011), pp. 127–128.

21. Y. Mei, D. J. Thurmer, C. Deneke, S. Kiravittaya, Y.-F. Chen, A. Dadgar, F. Bertram, B. Bastek, A. Krost, J. Christen, T. Reindl, M. Stoffel, E. Coric, and O. G. Schmidt, "Fabrication, self-assembly, and properties of ultrathin AlN/GaN porous crystalline nanomembranes: tubes, spirals, and curved sheets," ACS Nano **3**(7), 1663–1668 (2009).
22. M. Yu, M. Huang, D. E. Savage, M. G. Lagally, and R. H. Blick, "Local-wetting-induced deformation of rolled-up Si/Si-Ge nanomembranes: a potential route for remote chemical sensing," IEEE Trans. Nanotechnol. **10**(1), 21–25 (2011).
23. Y. Mei, G. Huang, A. A. Solovev, E. B. Ureña, I. Mönch, F. Ding, T. Reindl, R. K. Y. Fu, P. K. Chu, and O. G. Schmidt, "Versatile approach for integrative and functionalized tubes by strain engineering of nanomembranes on polymers," Adv. Mater. (Deerfield Beach Fla.) **20**(21), 4085–4090 (2008).
24. W. Chern, H.-K. Tsai, and X. Li, unpublished.
25. W. Chern, K. Hsu, I. S. Chun, B. P. Azeredo, N. Ahmed, K.-H. Kim, J. M. Zuo, N. Fang, P. Ferreira, and X. Li, "Nonlithographic patterning and metal-assisted chemical etching for manufacturing of tunable light-emitting silicon nanowire arrays," Nano Lett. **10**(5), 1582–1588 (2010).
26. E. J. Smith, Z. Liu, Y. F. Mei, and O. G. Schmidt, "System investigation of a rolled-up metamaterial optical hyperlens structure," Appl. Phys. Lett. **95**(8), 083104 (2009).
27. E. J. Smith, Z. Liu, Y. Mei, and O. G. Schmidt, "Combined surface plasmon and classical waveguiding through metamaterial fiber design," Nano Lett. **10**(1), 1–5 (2010).
28. S. Schwaiger, M. Bröll, A. Krohn, A. Stemmann, C. Heyn, Y. Stark, D. Stickler, D. Heitmann, and S. Mendach, "Rolled-up three-dimensional metamaterials with a tunable plasma frequency in the visible regime," Phys. Rev. Lett. **102**(16), 163903 (2009).
29. E. J. Smith, S. Schulze, S. Kiravittaya, Y. Mei, S. Sanchez, and O. G. Schmidt, "Lab-in-a-tube: detection of individual mouse cells for analysis in flexible split-wall microtube resonator sensors," Nano Lett. **11**(10), 4037–4042 (2011).
30. I. S. Chun, K. Bassett, A. Challa, and X. Li, "Tuning the photoluminescence characteristics with curvature for rolled-up GaAs quantum well microtubes," Appl. Phys. Lett. **96**(25), 251106 (2010).
31. Z. Huang, N. Geyer, P. Werner, J. de Boor, and U. Gösele, "Metal-assisted chemical etching of silicon: a review," Adv. Mater. (Deerfield Beach Fla.) **23**(2), 285–308 (2011).
32. A. Challa, 2010 http://hdl.handle.net/2142/16181.
33. X. Li and P. W. Bohn, "Metal-assisted chemical etching in HF/H_2 O_2 produces porous silicon," Appl. Phys. Lett. **77**(16), 2572 (2000).
34. I. S. Chun, E. K. Chow, and X. Li, "Nanoscale three dimensional pattern formation in light emitting porous silicon," Appl. Phys. Lett. **92**(19), 191113 (2008).
35. P. Cendula, S. Kiravittaya, I. Mönch, J. Schumann, and O. G. Schmidt, "Directional roll-up of nanomembranes mediated by wrinkling," Nano Lett. **11**(1), 236–240 (2011).
36. Z. Tian, F. Li, Z. Mi, and D. V. Plant, "Controlled transfer of single rolled-up InGaAs–GaAs quantum-dot microtube ring resonators using optical fiber abrupt tapers," IEEE Photon. Technol. Lett. **22**(5), 311–313 (2010).

37. J. Yoon, S. Jo, I. S. Chun, I. Jung, H.-S. Kim, M. Meitl, E. Menard, X. Li, J. J. Coleman, U. Paik, and J. A. Rogers, "GaAs photovoltaics and optoelectronics using releasable multilayer epitaxial assemblies," Nature **465**(7296), 329–333 (2010).

38. N. Ohtani, K. Kishimoto, K. Kubota, S. Saravanan, Y. Sato, S. Nashima, P. Vaccaro, T. Aida, and M. Hosoda, "Uniaxial-strain-induced transition from type-II to type-I band configuration of quantum well microtubes," Physica E **21**(2–4), 732–736 (2004).

39. S. Mendach, R. Songmuang, S. Kiravittaya, A. Rastelli, M. Benyoucef, and O. G. Schmidt, "Light emission and wave guiding of quantum dots in a tube," Appl. Phys. Lett. **88**(11), 111120 (2006).

40. S. Mendach, S. Kiravittaya, A. Rastelli, M. Benyoucef, R. Songmuang, and O. G. Schmidt, "Bidirectional wavelength tuning of individual semiconductor quantum dots in a flexible rolled-up microtube," Phys. Rev. B **78**(3), 035317 (2008).

41. F. Li, Z. Mi, and S. Vicknesh, "Coherent emission from ultrathin-walled spiral InGaAs/GaAs quantum dot microtubes," Opt. Lett. **34**(19), 2915–2917 (2009).

42. K. Dietrich, C. Strelow, C. Schliehe, C. Heyn, A. Stemmann, S. Schwaiger, S. Mendach, A. Mews, H. Weller, D. Heitmann, and T. Kipp, "Optical modes excited by evanescent-wave-coupled PbS nanocrystals in semiconductor microtube bottle resonators," Nano Lett. **10**(2), 627–631 (2010).

43. Ch. Strelow, H. Rehberg, C. M. Schultz, H. Welsch, Ch. Heyn, D. Heitmann, and T. Kipp, "Optical microcavities formed by semiconductor microtubes using a bottlelike geometry," Phys. Rev. Lett. **101**(12), 127403 (2008).

44. F. Li and Z. Mi, "Multiwavelength rolled-up InGaAs/GaAs quantum dot microtube lasers," Proc. SPIE **7591**, 75910O (2010).

45. G. Huang, V. A. Bolaños Quiñones, F. Ding, S. Kiravittaya, Y. Mei, and O. G. Schmidt, "Rolled-up optical microcavities with subwavelength wall thicknesses for enhanced liquid sensing applications," ACS Nano **4**(6), 3123–3130 (2010).

46. F. Li, S. Vicknesh, and Z. Mi, "Optical modes in InGaAs/GaAs quantum dot microtube ring resonators at room temperature," Electron. Lett. **45**(12), 645–646 (2009).

47. C. Strelow, H. Rehberg, C. M. Schultz, H. Welsch, C. Heyn, D. Heitmann, and T. Kipp, "Spatial emission characteristics of a semiconductor microtube ring resonator," Physica E **40**(6), 1836–1839 (2008).

48. S. Mendach, O. Schumacher, C. Heyn, S. Schnüll, H. Welsch, and W. Hansen, "Preparation of curved two-dimensional electron systems in InGaAs/GaAs-microtubes," Physica E **23**(3–4), 274–279 (2004).

49. S. Mendach, O. Schumacher, H. Welsch, C. Heyn, W. Hansen, and M. Holz, "Evenly curved two-dimensional electron systems in rolled-up Hall bars," Appl. Phys. Lett. **88**(21), 212113 (2006).

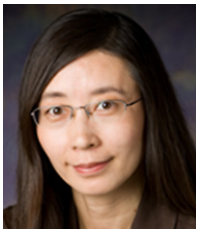

Xiuling Li received her Ph.D. degree from the University of California at Los Angeles. She joined the faculty of the University of Illinois in 2007, after working at a startup company for six years. She is currently an assistant professor in the Department of Electrical and Computer Engineering. Her current research interests are in the area of nanostructured semiconductor materials and devices. She has won the NSF CAREER award (2008), DARPA Young Faculty Award (2009), and ONR Young Investigator Award (2011). She has published over 60 journal papers. Her group's work on the planar nanowires has won one of the best student paper awards at the 2008 IEEE LEOS (now Photonic Society) annual meeting. The microtube and nanotube work has been identified as an outstanding symposium paper presented at the 2008 MRS meeting.